

Quasicrystals as a Hierarchy of Clusters

C. Janot¹ and M. de Boissieu²

¹*Institut Laue-Langevin, B.P. 156, 38042 Grenoble Cedex 9, France*

²*Laboratoire de Thermodynamique et de Physico-Chimie Métallurgiques, Ecole Nationale Supérieure d'Electronique et d'Electromécanique de Grenoble, B.P. 75, 38402 St. Martin d'Hères Cedex, France*

(Received 22 June 1993)

Diffraction approaches suggest that some quasicrystal structures can be described as hierarchical packing of atomic clusters. When treated as spherical potentials, these clusters may contain "magic numbers" of electrons which allow exact filling of the electronic shells of the hierarchy of wells. Physical properties such as high resistivity and diamagnetism are consistent with the model. Formation of quasicrystals at very critical composition is also explained.

PACS numbers: 61.44.+p, 71.30.+h

So far, experimental specification of quasicrystal structure has not reached the accuracy level currently achieved in regular crystallography [1]. However, the main features of these structures have been obtained via diffraction experiments, up to about 90% of the atomic positions, for perfect icosahedral quasicrystals of the Al-FeCu [2] and AlPdMn [3] systems. The average structure of the phason strained AlLiCu [4,5] quasicrystal has been determined as well, though within a lower accuracy level.

As an example, let us consider the atomic structure of AlPdMn quasicrystal [3] as obtained from neutron and x-ray diffraction. The basic elements of the structure are atomic clusters called pseudo-Mackay icosahedra (PMI) [3]. The PMI combine into τ^3 times as large inflated PMI of elementary PMI, and so on *ad infinitum* ($\tau = 2\cos 36^\circ$ is the golden mean) in such a way that the centers of the PMI, at any inflation step, are arranged in exactly the same fashion as the centers of the previous PMI generation, only scaled up by the τ^3 inflation factor. The elementary PMI are made of an external shell of 42 atoms (12 vertices of an icosahedron plus 30 vertices of an icosidodecahedron) and an inner shell of 8 or 9 atoms distributed on sites of a small dodecahedron. Contrary to the regular Mackay icosahedron, which has a full icosahedral symmetry, the PMI individually depart from that symmetry because of the partially occupied small dodecahedron.

Two types of PMI have been observed in the experimentally determined structure of the icosahedral quasicrystal AlPdMn [3]. One is basically a regular Mackay icosahedron with Mn atoms on the external icosahedron vertices and Al elsewhere, except for some substitution of a few Mn by Pd atoms. The other one contains about 20 Pd atoms and the rest is Al. Still according to diffraction data, the atoms and, subsequently, successive generation of PMI are connected along twofold and threefold bondings. Another experimental fact is the existence of "connecting units." These connecting units are pieces of PMI. They are arranged in shells having the same density as PMI [3] and can be looked at as "interfaces" in between the PMI. These interfaces also obey the inflation rules of the PMI. They are quite thick and contain about 37% of

the total volume ($\sim 1 - 50/\tau^9$) to be compared to the 30% atoms of the clusters which lie on their surfaces, accounting for all inflation levels.

The main drawback of this experimentally determined structure is that the exact composition of each PMI is not known. We maintain that basically the structure of AlPdMn is a skeleton made of τ^3 -inflated PMI packing. This is a little too simplistic but we have no more information so far. First order PMI have a diameter of about 10 Å and their centers are about 20 Å apart. It is assumed that the electronic density is homogeneous through the sample and equal to its average value. The same scheme roughly applied also to the experimentally determined structure of the AlFeCu icosahedral quasicrystal [2]. In the AlLiCu system, the structure [4,5] also shows atomic clusters in the form of small (ST) and large (LT) triacontahedra. Interestingly PMI, ST, and LT have equal atomic densities of 0.0656 atom/Å³ which is also fully consistent with measured densities [3,4].

The occurrence of icosahedral short range order (ISRO) in condensed matter is not surprising. Computer simulation on simple Lennard-Jones potentials confirmed that ISRO should be energetically favored [6]. Further evidence comes from the identification of special numbers in the mass spectra of *free* atomic cluster beams, corresponding to icosahedrally ordered atomic aggregates [7]. In these free atomic cluster beams the total numbers of "free" electrons must also be certain "magic numbers." A semiquantitative interpretation of these electron magnetic numbers has been deduced from a very simple model [8,9]. If the aggregates are stable, this means that electrons are trapped in a deep potential well induced by the positive ions of the cluster. In an extreme simplification, such an aggregate may be viewed as a deep spherical square well whose Schrödinger equation reduces to a Bessel equation. The energy eigenvalues are then given by

$$E_{n,l} = \frac{\hbar^2}{2\mu a^2} \chi_{n,l}^2, \quad (1)$$

in which n, l are the usual quantum numbers, μ is the electron mass, a the well radius, and $\chi_{n,l}$ are the zeros of the Bessel functions $J_{l+1/2}(kr)$. The occupation numbers

define the so-called electron “magic numbers” M . They have indeed been observed in free atomic aggregates [8,9] (Fig. 1). The cluster geometry induces roughly a Lorentzian broadening of the level, leading to densities of state which are in good agreement with the results of tight bonding calculations [10] [see the first large feature of $n(E)$ in Fig. 2]. If magic numbers of electrons give rise to stable, rare-gas-like, free aggregates, one may assume that slightly different numbers of electrons per aggregate will produce “connecting clusters” for the same reasons that non-rare-gas atoms do. This is just considering that atom aggregates behave like giant atoms.

A particular situation may arise if the number of electrons per cluster is equal to a magic number plus the exact average number n of electrons per atom. The inflated cluster (a cluster of N clusters, N being the number of atoms in the elementary cluster) will then dispose of the same magic number of electrons to stabilize itself. In order to go beyond we must dispose of the same number of exceeding electrons after each inflation step. Thus, we have enough electrons to stabilize the currently inflated cluster *and* initiate the forthcoming step of inflation *ad infinitum*. The condition can be expressed as

$$n = \frac{M}{N} \left(1 + \frac{1}{N} + \frac{1}{N^2} + \dots \right)$$

or

$$n = M/N - 1. \tag{2}$$

Thus, the composition for the structure to grow is very critical.

Actually, the model must be considered in its real dynamical image. It is indeed assumed that the elemen-

tary PMI clusters confine electrons like a spherical square well, with potential barriers around it. Electrons tunnel through these barriers. This can be approximated as hopping within the cluster of the next stage of inflation which in turn confines electrons in an inflated spherical square well, and so on. At each inflation stage electrons are confined by a barrier across which tunneling is harder and harder. In other words, the effective mass increases at each stage of the inflation hierarchy. The model proposes to account for such a “hierarchical tunneling” by stating that only a hierarchically decaying fraction of electrons per atom is allowed to freely leave the well states of a given stage of inflation to fill those of the next stage. Each cluster, at any stage of inflation, constantly keeps an average number of electrons equal to M to stabilize itself, via intercluster exchanges.

The electron density of state $n(E)$ of the built hierarchical structure can be roughly inferred by considering the succession of inflated spherical square wells attached to the successive generations of aggregates. The resulting atomic potential can then be viewed as a deep well whose bottom is a three-dimensional surface with hierarchical roughness: The narrowest and deepest wells are gathered into groups of N on the floor of τ^6 wider, τ^3 less deep wells which in turn are similarly distributed into even wider and less deep wells and so on. The τ^6 and τ^3 scale factors come from the inflation growth. The cluster, and then the attached spherical square well, have a radius which inflates with the scale factor τ^3 . This in turn forces the number of electronic states per atom specifically attributed to a cluster to decrease with the scale factor τ^9 and the corresponding energy “band” to extend over a width decaying with the scale factor [see Eq. (1)]. Then, the average number of electronic states per atom and per energy unit decreases with the scale factor τ^3 .

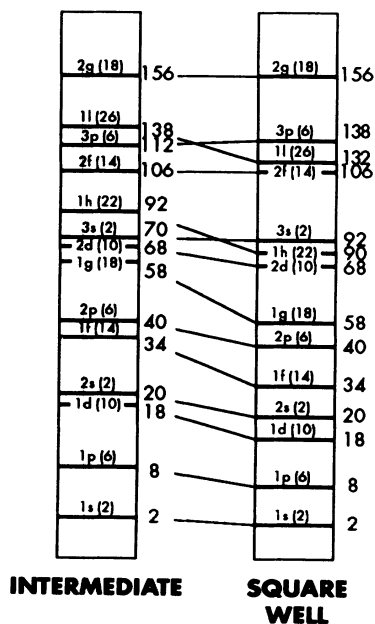


FIG. 1. Energy-level occupations for three-dimensional spherical wells [8].

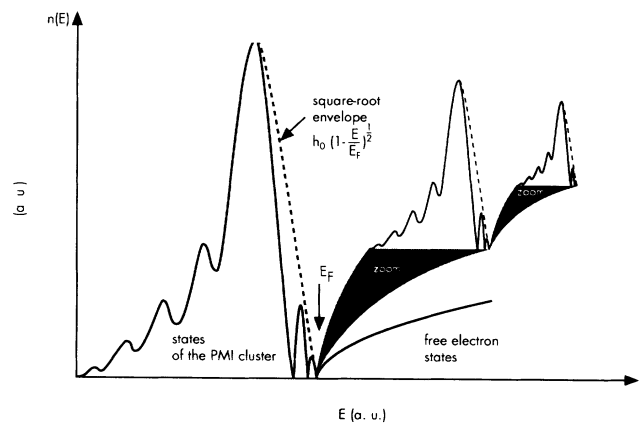


FIG. 2. Schematized density of electronic states. The large feature on the left hand side is the contribution of the elementary PMI. Features coming from the successive inflated PMI are simplified for the drawing. Zooming at E_F gives a flavor of the self-similar decay of the density of states. The dashed line is a square-root envelope of the main maxima in the successive cluster feature of $n(E)$.

The total density of states is qualitatively obtained by adding the "bonded" states of each well generation, the unbounded states of one generation falling into the bonded states of the next generation. This total density of states will thus show the density of states of the basic clusters on the low energy side, completed by successive similar features with areas reduced by cumulating scale factor τ^9 (τ^6 in extension, τ^3 in height) with deep pseudogaps in between. The density of states roughly converges as τ^{-3} up to a Fermi surface like the cutoff given by the geometric sum

$$E_F = \Delta E_0 \sum_{n=0}^{\infty} \frac{1}{\tau^{6n}} = \Delta E_0 \frac{\tau^6}{\tau^6 - 1} = 1.0590 \Delta E_0, \quad (3)$$

in which ΔE_0 is the full extension of the density of states for the basic PMI. It is easy to realize that only the very first features have significant surfaces, as illustrated in Fig. 2. Beyond that, the density of states degenerates into a dense piling up of very narrow features, reasonably mimicked by a short tail decaying toward E_F , following an equation given by

$$n(E) = n_0 / \tau^{3p}, \quad E = \Delta E_0 \sum_{n=0}^p \frac{1}{\tau^{6n}}, \quad (4)$$

i.e.,

$$n(E) = n_0 (1 - E/E_F)^{1/2}.$$

Empty states at 0 K are distributed into a free electron band [$n(E) \sim (E - E_F)^{1/2}$] (Fig. 2). On both sides of the Fermi level $n(E)$ increases as a square-root function of energy changes with respect to E_F . But the $n(E_F)$ valley is asymmetric as separating free electron states on one side (extended over a large energy range with a rather flat density) from semibonded states whose density increases sharply on the other side. The width of the pseudogaps is zero because the inflation mechanism continuously reduces the well deepness and then progressively degenerates the energy level into free states.

In summary, the global electron density of states exhibits a self-similar geometry and the Fermi surface has a fractal character. If the lowest energy pseudogap corresponding to the top of the first subband (electron states for elementary clusters) is typically situated at 10 eV, the Fermi level is only some 0.5901 eV beyond. The full width of the successive subbands rapidly falls from 10 eV to 0.5573, 0.0310, 0.0017, 0.0001, ... eV. Close to the Fermi level there is an infinity of decaying pseudodiscrete levels within an energy range smaller than 5×10^{-5} eV. Thus, at rather low energy excitation, say below 0.05 eV or so, one should observe some sort of semimetal-like behavior, with a square-root distribution of electronic states in both filled valence and empty conduction bands. For a slightly different composition that would allow cluster states to fill up to a certain stage of inflation only but not *ad infinitum*, the hierarchy would be interrupted at some energy and the Fermi level fall somewhere within the valence band. This generates approximant periodic structure with the density of states at E_F scaling as $1/\tau^{3n}$.

The predictions of the models seem to be in good consistency with experimental observation [11–20]. At 0 K the present model is a perfect insulator and has diamagnetic behavior due to all electrons being in saturated states of the well hierarchy. The conductivity $\sigma(T)$ at $T=0$ K is not strictly zero for real quasicrystals but there is a clear trend to this ideal value as the quality of the samples improves [18–20]. Diamagnetism has actually been observed [16].

As temperature increases electrons are transferred from the bonding states to the conduction band. For $kT \leq 0.05$ eV, i.e., $T \leq 600$ K the number of free carriers (electrons in the conduction band and holes in the filled well band) can easily be calculated using the square-root shape of the density of states. One finds that the number of electrons in the conduction band increases as $T^{3/2}$. In this temperature range only the conduction band is conducting (electron conduction) since holes are created into flat bands with quite poor mobilities. At higher temperature, electrons from the state of the small clusters get excited as well and both valence and conduction bands are conducting. Thus, $\sigma(T)$ should roughly increase as $T^{3/2}$ up to $T \sim 600$ K and more rapidly above. This is pictured in Fig. 3 which compares experimental data [18] with the $T^{3/2}$ power law.

The analysis is also qualitatively valid to explain the sign changes in Hall constant and thermal power. At low temperature, free electron carriers (in small numbers) give weakly negative R_H and S . As T increases the flat small subbands in between the Fermi level and the upper part of the larger features of the density of states are progressively stripped from their electron, generating an effective pseudogap of increasing width. Thus, the behavior becomes that of a poor semiconductor with increasing energy gap $E_g(T)$ and then positive increasing $R_H(T)$, $S(T)$ values [12].

Within the same scheme, one can calculate the temperature dependence of the total electron energy and the electron contribution to heat capacity. This result is $\Delta E_{el} \propto T^{5/2}$ and, consequently $C_{el} \propto T^{3/2}$ (instead of T^2

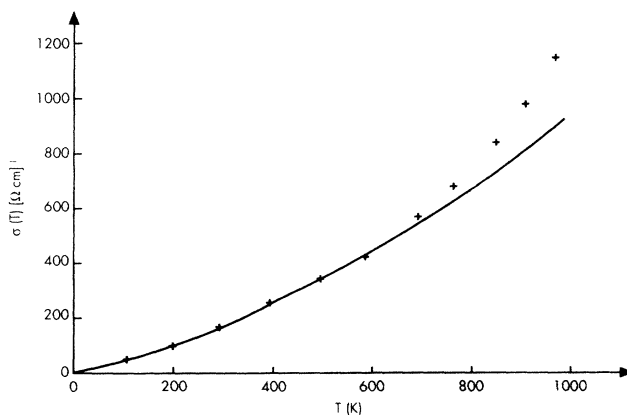


FIG. 3. Conductivity data [18] (+) compared with the $T^{3/2}$ power law (—).

and T , respectively, for a metal) in the low temperature range ($T \leq 600$ K). If so, the usual analysis of the heat capacity data in terms of a C/T vs T^2 curve would be irrelevant.

Finally, the experimental behavior of the optical conductivity is also rather well explained by the present model. At 0 K, the filled envelope of subbands just below the empty conduction band can produce optical absorption via the interband transition only. The optical conductivity σ_{op} may be expressed as

$$\sigma_{op} = \frac{c}{\omega^2} M^2 \text{ (JDS)},$$

where c is a constant. M a matrix element for the electron transition, and JDS, the joint density of states, can be approximated by the product of the number of states found in each of the two bands within an energy range equal to the photon energy $\hbar\omega$ on each side of E_F . A straightforward calculation, still with square-root envelopes, results in $\sigma_{op} \propto \hbar\omega$. Beyond a certain energy threshold, the two bands are expected to have enough empty and filled states in good proportion to permit intraband transition for a Drude-like behavior to be recovered. The linear $\sigma_{op}(\hbar\omega)$ dependence at low $\hbar\omega$ and the Drude decay on the high energy side have actually been observed [15].

Now, it also may be interesting to test Eq. (2) with respect to the composition of real quasicrystals. Within the example of the perfect stable quasicrystals, $\text{Al}_{0.62}\text{Cu}_{0.255}\text{Fe}_{0.125}$, $\text{Al}_{0.70}\text{Pd}_{0.22}\text{Mn}_{0.08}$, $\text{Al}_{70}\text{Pd}_{20}\text{Re}_{10}$, or $\text{Al}_{64}\text{Cu}_{22}\text{Ru}_{14}$, the assumed hierarchical structure is based on an averaged PMI cluster with 50.5 atoms each. In the above alloys the 60% to 70% of Al will bring about 100 electrons per PMI (valence +3). The valence +1 for Cu may also be accepted confidently. Transition metals in alloys have negative valences which, unfortunately, depend on the structure [21]. They should be strongly negative for the magic number to be 58 (see Fig. 1). Thus, we are left with $M=92$ in Eq. (2), which gives 1.86 e/atom . It is then possible to obtain the above real compositions if negative valences are close to -2 for Fe, Ru, Mn, and Re and close to -0.6 for Pd. In $\text{Al}_{0.570}\text{Cu}_{0.108}\text{Li}_{0.322}$ quasicrystals [22] there are 2.14 e/atom which would also correspond to $M=92$ in a ST cluster.

In conclusion, we have proposed to related stability and properties of quasicrystals to a description of their structure in terms of a hierarchy of aggregates. This is an extension of both the so-called compartmentalization analysis [23] and interband transitions via electronic hopping descriptions [18]. This is also consistent with theoretical calculations [24] in the sense that the reported confined states should correspond to electron density of states in the small clusters. The pseudogap effects are reproduced as well, directly related to physical concepts and in good agreement with spectroscopy data [25]. Owing to the very strong criticality, it may also be conjectured that exact chemical composition and local homo-

geneity cannot be easily satisfied in real alloys, which may result in "experimental quasicrystals" being actually mixtures of approximants rather than pure perfect quasicrystals.

-
- [1] C. Janot, *Quasicrystals: A Primer* (Oxford Univ. Press, New York, 1992).
 - [2] M. Cornier-Quiquandon, M. Quivy, S. Lefebvre, E. Elkaim, G. Heger, A. Katz, and D. Gratias, *Phys. Rev. B* **44**, 2071 (1991).
 - [3] M. Boudard, M. de Boissieu, C. Janot, G. Heger, C. Beeli, H.-U. Nissen, H. Vincent, R. Ibberson, M. Audier, and J. M. Dubois, *J. Phys. Condens. Matter* **4**, 10149 (1992); M. Boudard, thesis, Grenoble, 1993.
 - [4] M. de Boissieu, C. Janot, J. M. Dubois, M. Audier, and B. Dubost, *J. Phys. Condens. Matter* **3**, 1 (1991).
 - [5] M. de Boissieu, C. Janot, J. Pannetier, J. M. Dubois, M. Audier, and B. Dubost, *J. Phys. (Paris)* **50**, 1689 (1989).
 - [6] P. J. Steinhardt, D. R. Nelson, and M. Ronchetti, *Phys. Rev. B* **28**, 24 (1983).
 - [7] K. Sattler, J. Mühlbach, O. Eckt, P. Pfau, and E. Recknagel, *Phys. Rev. Lett.* **47**, 160 (1981).
 - [8] W. A. de Heer, W. D. Knight, M. Y. Chou, and M. L. Cohen, *Solid State Phys.* **40**, 93 (1987).
 - [9] T. P. Martin, T. Bergmann, H. Göhlich, and T. Lange, *J. Phys. Chem.* **95**, 6421 (1991).
 - [10] A. E. Carlsson and R. Phillips, in *Quasicrystals: The State of the Art*, edited by D. P. DiVincenzo and P. J. Steinhardt (World Scientific, Singapore, 1991), p. 361.
 - [11] T. Klein, C. Berger, D. Mayou, and F. Cyrot-Lackmann, *Phys. Rev. Lett.* **66**, 2907 (1991).
 - [12] B. D. Biggs, Y. Li, and S. J. Poon, *Phys. Rev. B* **43**, 8747 (1991).
 - [13] S. J. Poon, *Adv. Phys.* **41**, 303 (1992).
 - [14] P. Lanco, T. Klein, C. Berger, F. Cyrot-Lackmann, G. Fourcaudot, and A. Sulpice, *Europhys. Lett.* **18**, 227 (1992).
 - [15] C. C. Homes, T. Timusk, X. Wu, Z. Attounian, A. Sahnoune, and J. O. Ström-Olsen, *Phys. Rev. Lett.* **67**, 2694 (1991).
 - [16] T. Klein *et al.*, *Phys. Rev. B* **45**, 2049 (1992).
 - [17] M. A. Howson and B. L. Gallagher, *Phys. Rep.* **170**, 265 (1988).
 - [18] D. Mayou, C. Berger, F. Cyrot-Lackmann, T. Klein, and P. Lanco, *Phys. Rev. Lett.* **70**, 3915 (1993).
 - [19] F. S. Pierce, S. J. Poon, and B. D. Biggs, *Phys. Rev. Lett.* **70**, 3919 (1993).
 - [20] F. S. Pierce, S. J. Poon, and B. D. Biggs, *Science* **261**, 737 (1993).
 - [21] J. Friedel, *Philos. Mag.* **B 65**, 1125 (1992).
 - [22] B. Dubost, C. Colinet, and J. Ansara, in *Quasicrystalline Materials*, edited by C. Janot and J. M. Dubois (World Scientific, Singapore, 1988).
 - [23] J. C. Phillips and K. Rabe, *Phys. Rev. Lett.* **66**, 923 (1991); J. C. Phillips, *Solid State Commun.* **83**, 379 (1992).
 - [24] T. Fujiwara and H. Tsunetsugu, in *Quasicrystals: The State of the Art* (Ref. [10]), p. 343.
 - [25] E. Belin, Z. Dankhazit, A. Sadoc, Y. Calvayrac, T. Klein, and J. M. Dubois, *J. Phys. Condens. Matter.* **4**, 4459 (1992).

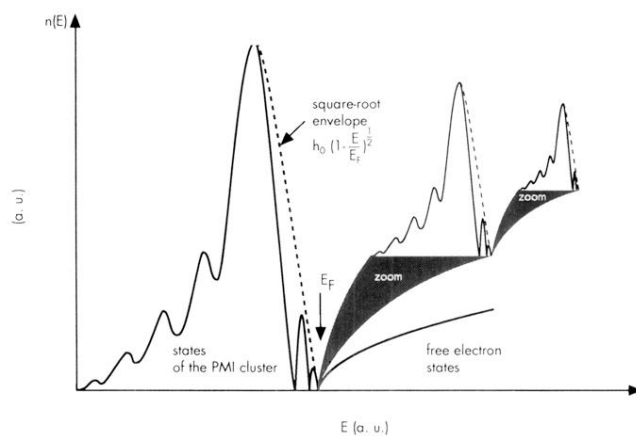


FIG. 2. Schematized density of electronic states. The large feature on the left hand side is the contribution of the elementary PMI. Features coming from the successive inflated PMI are simplified for the drawing. Zooming at E_F gives a flavor of the self-similar decay of the density of states. The dashed line is a square-root envelope of the main maxima in the successive cluster feature of $n(E)$.